

**Noise breaking the twofold symmetry of photosynthetic reaction centers: Electron transfer**

Richard Pinčák

*Department of Biophysics, P.J. Šafárik University, Jesenná 5, 041 54 Košice, Slovak Republic*

Michal Pudlak\*

*Institute of Experimental Physics, Slovak Academy of Sciences, Watsonova 47, 043 53 Košice, Slovak Republic*

(Received 17 May 2000; revised manuscript received 27 March 2001; published 29 August 2001)

In this work we present a stochastic model to elucidate the unidirectionality of the primary charge separation process in the bacterial reaction centers where two symmetric ways of electron transfer (ET), starting from the common electron donor, are possible. We have used a model of three sites/molecules with ET beginning at site 1 with the option to proceed to site 2 or site 3. If the direct ET between sites 2 and 3 is not allowed and electron cannot escape from the system then it is shown that the different stochastic fluctuations in the energy of sites and the interaction between sites on these two ways are sufficient to cause the transient asymmetric electron distribution at site 2 and 3 during relaxation to the steady state. This means that overall asymmetric ET can be caused by the transient asymmetric electron distribution if there is a possibility for an electron to escape from the three-site system. To explore this possibility we have introduced a sink into the model at the end of each of the sites 2 and 3. The dependence of the asymmetry in electron transfer on the value of the sink parameter, introduced through an additional imaginary diagonal matrix element of the Hamiltonian, was investigated. Results show indeed that the unidirectionality of the electron transfer generated in the system of three molecules depends strongly on the sink parameter value.

DOI: 10.1103/PhysRevE.64.031906

PACS number(s): 87.10.+e, 87.15.Rn, 87.16.Uv, 82.20.Fd

**I. INTRODUCTION**

The crystallization of a bacterial reaction center protein and elucidation of its structure open the door to the understanding of the conversion of solar energy in usable chemical energy on the microscopic level [1,2]. The photosynthetic reaction center [3] is a special pigment-protein complex, that functions as a photochemical trap. The precise details of the charge separations reactions and subsequent dark electron transport form the central question of the conversion of solar energy into the chemical energy of photosynthetic organism.

The reaction centers (RCs) of a purple bacteria are composed of three protein subunits called  $L$ ,  $M$ , and  $H$  [4,5]. All cofactors involved in the electron transfer (ET) are noncovalently bound to subunits  $L$  and  $M$  in two chains. Both chains of cofactors start at the bacteriochlorophyll dimer ( $P$ ) that interacts with both subunits  $L$  and  $M$ . Then the cofactor chains are split and each individual one continues on subunit  $L$  and symmetrically on subunit  $M$ . Cofactors in subunit  $L$  are accessory bacteriochlorophyll (BChl $_L$ ), bacteriopheophytin (BPh $_L$ ) and quinone ( $Q_L$ ). Identically in the  $M$  subunit are the accessory bacteriochlorophyll (BChl $_M$ ), bacteriopheophytin (BPh $_M$ ) and quinone ( $Q_M$ ). The arrangement of cofactors shows the local twofold symmetry which is almost perfect in the arrangement to the bacteriochlorophyll dimer. The part of the  $L$  subunit involved in ET can be superimposed onto the corresponding part of the  $M$  subunit by a rotation of almost exactly 180°. For more details on structural arrangement, see Ref. [6].

The cofactors serve as donor-acceptor pairs in the electron transfer. In spite of the structural symmetry, the RC is func-

tionally highly asymmetric. In the primary charge transfer an electron is transferred from photoexcited special pair  $P$ , the starting point for a series of electron transfer reactions across the membrane, to the cofactors on subunit  $L$ , to BChl $_L$ , BPh $_L$ ,  $Q_L$ , and  $Q_M$  [7,8]. On the other hand, the chain located on subunit  $M$  is inactive in ET. The highly asymmetric functionality, however, can be decreased by amino acid mutations or cofactor modification [9].

Our understanding of the primary processes in photosynthesis is not complete without explanation of the strong asymmetry in ET. We believe that the reason for asymmetric ET between prosthetic groups located on different polypeptides is a different molecular dynamics. Dynamics of atoms causes the change of the electrical potential fields and the conformational variations influence the mutual orientations between cofactors. Then the energy gap and overlap of electronic wave functions fluctuates as a result in the system. The net result is a different fluctuation of electronic energy levels on prosthetic groups and also a different fluctuation of the overlaps of the electronic wave functions on  $L$  and  $M$  branches. This approach can be used to explain the effect of individual amino acid mutation or cofactor modifications on the observed balance between the forward ET reaction on the  $L$  side of the RC, the charge recombination processes, and ET to the  $M$ -side chromophores [9–13].

**II. MODEL FOR ASYMMETRIC ET**

To describe the first steps of electron transfer processes in the reaction centers we have used the three-site model. The model is basically an extension of the theory of coupled motion of a quantum particle in a fluctuating medium [14–24]. Let us designate the special pair ( $P$ ) as site 1; sites 2 and 3 then represent the first molecules on branches  $M$  and  $L$ .

\*Email address: pudlak@saske.sk

Because of symmetry we assume that both local energies at 2 (branch  $M$ ) and 3 (branch  $L$ ) and the hopping terms between molecule 1 and molecule 2 or 3 on both branches are also the same. We forbid the direct ET between sites 2 and 3 and consider that this three level system is coupled stochastically to a bath with white noise. We assume that energy levels 2 and 3 have an imaginary part which describes the interaction with the next molecule in the branch. The meaning of the imaginary part is the lifetime of electron localization at site 2 or 3 in the limit when hopping terms are zero [22]. The imaginary part of energy level 1 describes the probability of electron deactivation to the ground state. Then the Hamiltonian of our model has the form

$$H = \sum_{k=1}^3 E_k a_k^+ a_k + \sum_{i=2,3} [J + \alpha_i(t)] (a_i^+ a_1 + \text{H.c.}), \quad (1)$$

where  $J$  is the electronic coupling parameter (hopping term). The  $E_i$  and  $a_i^+$  ( $a_i$ ) are the site energy and the creation (annihilation) operator of the electron at site  $i$ , correspondingly. The terms  $\alpha_i$  represent stochastic fluctuations of electronic coupling parameter. We assume that

$$E_1 = \varepsilon_1 - i\Gamma_1, \quad (2a)$$

$$E_2 = \varepsilon_2 - i\Gamma_2 + \beta_2(t), \quad (2b)$$

$$E_3 = \varepsilon_3 - i\Gamma_3 + \beta_3(t). \quad (2c)$$

Here  $\beta_i$  represents stochastic fluctuations in the energy at site  $i$ . The parameter  $\hbar/2\Gamma_i$  has a meaning of the lifetime of the electron localization at site  $i$  in the limit of the zero coupling parameter. Our assumption about stochastic functions is that

$$\langle \beta_k(t) \rangle = \langle \alpha_i(t) \rangle = 0 \quad (3)$$

and different from zero are only following correlation functions:

$$\langle \alpha_i(t) \alpha_i(\tau) \rangle = \Delta_i \delta(t - \tau), \quad i = 2, 3, \quad (4a)$$

$$\langle \beta_k(t) \beta_k(\tau) \rangle = \mu_k \delta(t - \tau), \quad k = 2, 3. \quad (4b)$$

$\langle \rangle$  denotes the statistical ensemble average. Relations (4) imply that the fluctuations at different times are uncorrelated and correspond to the shortest correlation time limit of a Gaussian-Markov process.

The main goal of the present work is to compute the rate of quantum yield  $\Phi_3$  and  $\Phi_2$  of the electron escape via the branch  $L$  (site 3) and  $M$  (site 2). We start from the Liouville equation

$$i\hbar \frac{\partial \rho}{\partial t} = [H\rho - \rho H^+]. \quad (5)$$

In the matrix form we get

$$i\hbar \partial_t \rho_{11} = [J + \alpha_2(t)](\rho_{21} - \rho_{12}) + (J + \alpha_3)(\rho_{31} - \rho_{13}) - 2i\Gamma_1 \rho_{11}, \quad (6a)$$

$$i\hbar \partial_t \rho_{12} = [J + \alpha_2(t)](\rho_{22} - \rho_{11}) + [\varepsilon_1 - \varepsilon_2 - i\Gamma_1 - i\Gamma_2 - \beta_2(t)]\rho_{12} + [J + \alpha_3(t)]\rho_{32}, \quad (6b)$$

$$i\hbar \partial_t \rho_{21} = [J + \alpha_2(t)](\rho_{11} - \rho_{22}) + [\varepsilon_2 + \beta_2(t) - i\Gamma_2 - i\Gamma_1 - \varepsilon_1]\rho_{21} - [J + \alpha_3(t)]\rho_{23}, \quad (6c)$$

$$i\hbar \partial_t \rho_{22} = [J + \alpha_2(t)](\rho_{12} - \rho_{21}) - 2i\Gamma_2 \rho_{22}, \quad (6d)$$

$$i\hbar \partial_t \rho_{13} = [J + \alpha_3(t)](\rho_{33} - \rho_{11}) + [\varepsilon_1 - \varepsilon_3 - i\Gamma_1 - i\Gamma_3 - \beta_3(t)]\rho_{13} + [J + \alpha_2(t)]\rho_{23}, \quad (6e)$$

$$i\hbar \partial_t \rho_{31} = -[J + \alpha_3(t)](\rho_{33} - \rho_{11}) - [\varepsilon_1 - \varepsilon_3 + i\Gamma_3 + i\Gamma_1 - \beta_3(t)]\rho_{31} - [J + \alpha_2(t)]\rho_{32}, \quad (6f)$$

$$i\hbar \partial_t \rho_{23} = [\varepsilon_2 - \varepsilon_3 + \beta_2(t) - \beta_3(t) - i\Gamma_2 - i\Gamma_3]\rho_{23} - [J + \alpha_3(t)]\rho_{21} + [J + \alpha_2(t)]\rho_{13}, \quad (6g)$$

$$i\hbar \partial_t \rho_{32} = -[\varepsilon_2 - \varepsilon_3 + \beta_2(t) - \beta_3(t) + i\Gamma_2 + i\Gamma_3]\rho_{32} + [J + \alpha_3(t)]\rho_{12} - [J + \alpha_2(t)]\rho_{31}, \quad (6h)$$

$$i\hbar \partial_t \rho_{33} = -2i\Gamma_3 \rho_{33} + [J + \alpha_3(t)](\rho_{13} - \rho_{31}). \quad (6i)$$

The averaging (6) gives the terms  $\langle \alpha_k \rho_{ij} \rangle$ ,  $\langle \beta_k \rho_{ij} \rangle$ . To split these terms we use the Furutsu-Novikov relation [25–27]

$$\langle \alpha_k \rho_{ij} \rangle = \sum_{\lambda=\alpha}^{\beta} \sum_{l=2}^3 \int d\tau \langle \alpha_k(t) \lambda_l(\tau) \rangle \left\langle \frac{\partial \rho_{ij}(t)}{\partial \lambda_l(\tau)} \right\rangle, \quad (7a)$$

$$\langle \beta_k \rho_{ij} \rangle = \sum_{\lambda=\alpha}^{\beta} \sum_{l=2}^3 \int d\tau \langle \beta_k(t) \lambda_l(\tau) \rangle \left\langle \frac{\partial \rho_{ij}(t)}{\partial \lambda_l(\tau)} \right\rangle. \quad (7b)$$

Then we have

$$\begin{aligned} \partial_t \langle \rho_{11} \rangle &= -i \frac{J}{\hbar} (\langle \rho_{21} \rangle - \langle \rho_{12} \rangle + \langle \rho_{31} \rangle - \langle \rho_{13} \rangle) \\ &\quad - \frac{2\Delta_2}{\hbar^2} (\langle \rho_{11} \rangle - \langle \rho_{22} \rangle) \\ &\quad - \frac{2\Delta_3}{\hbar^2} (\langle \rho_{11} \rangle - \langle \rho_{33} \rangle) - \frac{2\Gamma_1}{\hbar} \langle \rho_{11} \rangle, \end{aligned} \quad (8a)$$

$$\begin{aligned} \partial_t \langle \rho_{12} \rangle &= -\frac{\Gamma_1 + \Gamma_2}{\hbar} \langle \rho_{12} \rangle - i \frac{\varepsilon_1 - \varepsilon_2}{\hbar} \langle \rho_{12} \rangle \\ &\quad - i \frac{J}{\hbar} (\langle \rho_{22} \rangle - \rho_{11} + \langle \rho_{32} \rangle) \\ &\quad + \frac{2\Delta_2}{\hbar^2} (\langle \rho_{21} \rangle - \langle \rho_{12} \rangle) - \frac{\mu_2 + \Delta_3}{\hbar^2} \langle \rho_{12} \rangle, \end{aligned} \quad (8b)$$

$$\begin{aligned} \partial_t \langle \rho_{21} \rangle = & -\frac{\Gamma_1 + \Gamma_2}{\hbar} \langle \rho_{21} \rangle + i \frac{\varepsilon_1 - \varepsilon_2}{\hbar} \langle \rho_{21} \rangle \\ & + i \frac{J}{\hbar} (\langle \rho_{22} \rangle - \langle \rho_{11} \rangle + \langle \rho_{23} \rangle) \\ & + \frac{2\Delta_2}{\hbar^2} (\langle \rho_{12} \rangle - \langle \rho_{21} \rangle) - \frac{\mu_2 + \Delta_3}{\hbar^2} \langle \rho_{21} \rangle, \end{aligned} \quad (8c)$$

$$\begin{aligned} \partial_t \langle \rho_{22} \rangle = & -\frac{2\Gamma_2}{\hbar} \langle \rho_{22} \rangle + \frac{2\Delta_2}{\hbar^2} (\langle \rho_{11} \rangle - \langle \rho_{22} \rangle) \\ & - i \frac{J}{\hbar} (\langle \rho_{12} \rangle - \langle \rho_{21} \rangle), \end{aligned} \quad (8d)$$

$$\begin{aligned} \partial_t \langle \rho_{13} \rangle = & -\frac{\Gamma_1 + \Gamma_3}{\hbar} \langle \rho_{13} \rangle - i \frac{\varepsilon_1 - \varepsilon_3}{\hbar} \langle \rho_{13} \rangle \\ & - i \frac{J}{\hbar} (\langle \rho_{33} \rangle - \langle \rho_{11} \rangle + \langle \rho_{23} \rangle) \\ & - \frac{\mu_3 + \Delta_2}{\hbar^2} \langle \rho_{13} \rangle - \frac{2\Delta_3}{\hbar^2} (\langle \rho_{13} \rangle - \langle \rho_{31} \rangle), \end{aligned} \quad (8e)$$

$$\begin{aligned} \partial_t \langle \rho_{31} \rangle = & -\frac{\Gamma_1 + \Gamma_3}{\hbar} \langle \rho_{31} \rangle + i \frac{\varepsilon_1 - \varepsilon_3}{\hbar} \langle \rho_{31} \rangle \\ & + i \frac{J}{\hbar} (\langle \rho_{33} \rangle - \langle \rho_{11} \rangle + \langle \rho_{32} \rangle) \\ & - \frac{\mu_3 + \Delta_2}{\hbar^2} \langle \rho_{31} \rangle + \frac{2\Delta_3}{\hbar^2} (\langle \rho_{13} \rangle - \langle \rho_{31} \rangle), \end{aligned} \quad (8f)$$

$$\begin{aligned} \partial_t \langle \rho_{23} \rangle = & -\frac{\Gamma_2 + \Gamma_3}{\hbar} \langle \rho_{23} \rangle + i \frac{\varepsilon_3 - \varepsilon_2}{\hbar} \langle \rho_{23} \rangle \\ & - i \frac{J}{\hbar} (\langle \rho_{13} \rangle - \langle \rho_{21} \rangle) \\ & - \frac{\mu_2 + \mu_3 + \Delta_2 + \Delta_3}{\hbar^2} \langle \rho_{23} \rangle, \end{aligned} \quad (8g)$$

$$\begin{aligned} \partial_t \langle \rho_{32} \rangle = & -\frac{\Gamma_2 + \Gamma_3}{\hbar} \langle \rho_{32} \rangle - i \frac{\varepsilon_3 - \varepsilon_2}{\hbar} \langle \rho_{32} \rangle \\ & + i \frac{J}{\hbar} (\langle \rho_{31} \rangle - \langle \rho_{12} \rangle) \\ & - \frac{\mu_2 + \mu_3 + \Delta_2 + \Delta_3}{\hbar^2} \langle \rho_{32} \rangle, \end{aligned} \quad (8h)$$

$$\begin{aligned} \partial_t \langle \rho_{33} \rangle = & -\frac{2\Gamma_3}{\hbar} \langle \rho_{33} \rangle - i \frac{J}{\hbar} (\langle \rho_{13} \rangle - \langle \rho_{31} \rangle) \\ & + \frac{2\Delta_3}{\hbar^2} (\langle \rho_{11} \rangle - \langle \rho_{33} \rangle). \end{aligned} \quad (8i)$$

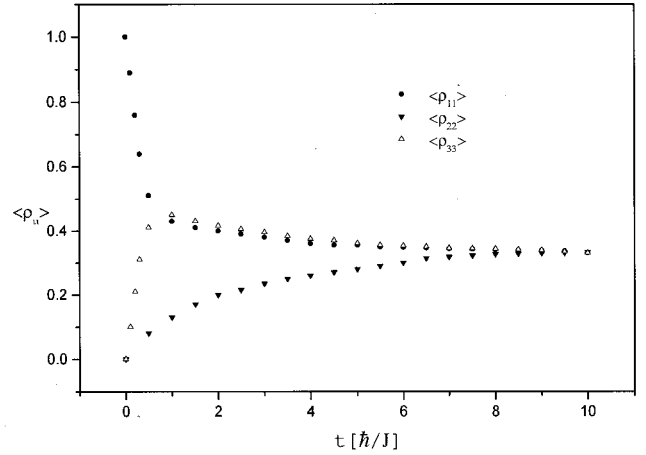


FIG. 1. The time dependence of the site-occupation probabilities  $\rho_{il}(t)$  for the sites  $l=1,2,3$ . The following parameters were used:  $J=1$ ,  $\Gamma=0$ ,  $\varepsilon_2=10$ ,  $\varepsilon_3=10$ ,  $\mu_2/\hbar=2$ ,  $\mu_3/\hbar=8$ ,  $\Delta_2/\hbar=0.1$ ,  $\Delta_3/\hbar=1$ .  $J$  is a hopping term;  $\varepsilon_i$  are the site energies;  $\mu_i$  and  $\Delta_i$  are characterizing the energy level fluctuation and the fluctuations of hopping term at site  $i$ , respectively.  $\Gamma$  describes the possibility of electronic escape from the system of three molecules. Time is in  $\hbar/J$  units and the other parameters are in  $J$  units.

Throughout the paper, with the exception of Sec. V, we assume that  $\Gamma_1=0$  and  $\Gamma_2=\Gamma_3=\Gamma$ . In the computations of Eq. (8) we put  $\varepsilon_1=0$ . The numerical solution of this set of differential equations both for  $\Gamma$  equal to and not equal to zero is presented in Figs. 1 and 2. In both cases we start with an electron initially localized at site 1. The behavior of the system depends strongly on the fluctuation of the parameters. For the case of  $\Gamma_1=\Gamma_2=\Gamma_3=0$  (Fig. 1) the probability to find an electron at site 1 is decreasing with the elapsed time. However, the probability to find electron at site 2 and 3 increases asymmetrically. At site 2 the probability is slowly approaching the value of  $\frac{1}{3}$  in a long time scale. The different behavior is observed at site 3. At this site the probability rapidly rises and at some specific time it has a value greater

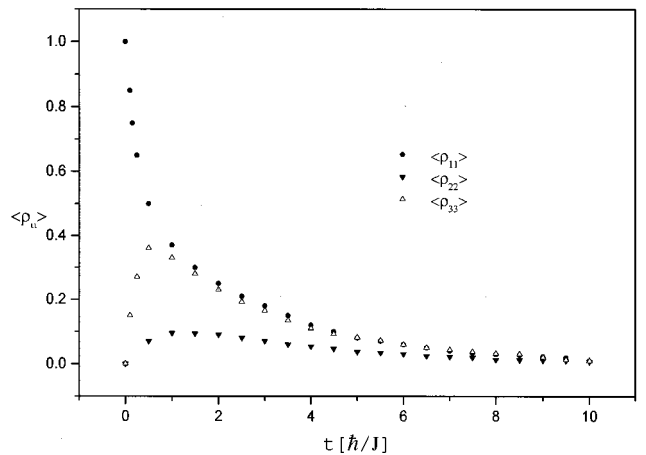


FIG. 2. The time dependence of the site-occupation probabilities  $\langle \rho_{il}(t) \rangle$  for the sites  $l=1,2,3$ . The parameters used were:  $J=1$ ,  $\Gamma=0.3$ ,  $\varepsilon_2=10$ ,  $\varepsilon_3=10$ ,  $\mu_2/\hbar=2$ ,  $\mu_3/\hbar=8$ ,  $\Delta_2/\hbar=0.1$ ,  $\Delta_3/\hbar=1$ . Units are as described in the legend of Fig. 1.

than  $\frac{1}{3}$  and with elapsing time it relaxes to  $\frac{1}{3}$ . This kind of overall transition to the steady state we call the asymmetric relaxation. The final steady state distribution is equal for each site because the noise does not depend on the localization of the electron. The similar results were obtained earlier for the two states model [25,28]. We can also see that the unidirectionality of the electron transfer generated in the system of three molecules may depend on the next step of electron transport (Fig. 1). It means that it depends on the probability of electronic escape from the system. We will assume that this probability is equal for branches  $L$  and  $M$ . To characterize this probability we have included the parameter  $\Gamma$  to the model. It is an *ad hoc* generalization of the Wigner-Weisskopf exponential decay law [29]. The solution of Eqs. (8) with  $\Gamma$  different from zero is presented in Fig. 2. The integral below the curve  $\langle \rho_{22}(t) \rangle$  [ $\langle \rho_{33}(t) \rangle$ ] characterizes the possibility of the electronic escape through branch  $M$  ( $L$ ). Time is measured in the units  $\hbar/J$ .

### III. CALCULATION OF ELECTRONIC ESCAPE THROUGH THE BRANCHES

The quantum yield  $\Phi_i$  of the electronic escape via site  $i$  can be characterized by the expression

$$\Phi_i = \frac{2\Gamma_i}{\hbar} \int_0^\infty \langle \rho_{ii}(t) \rangle dt = \frac{2\Gamma_i}{\hbar} \lim_{p \rightarrow 0^+} \langle \tilde{\rho}_{ii}(p) \rangle, \quad i = 1, 2, 3, \quad (9)$$

where  $\langle \tilde{\rho}_{ii}(p) \rangle$  is the Laplace transformation of  $\langle \rho_{ii}(t) \rangle$ . The quantum yields  $\Phi_i$  must fulfil the expression

$$\Phi_1 + \Phi_2 + \Phi_3 = 1.$$

It means that electrons can escape from the system through branch  $L$  or  $M$  or the system decay to the ground state which characterized the quantity  $\Phi_1$ . Assuming the initial conditions

$$\langle \rho_{11}(0) \rangle = 1, \quad \langle \rho_{22}(0) \rangle = \langle \rho_{33}(0) \rangle = 0$$

we can solve Eqs. (8) in Laplace transformation. For our goal the main importance is parameter  $K$ ,

$$K = \frac{\Phi_3}{\Phi_2} = \frac{\langle \tilde{\rho}_{33}(p \rightarrow 0) \rangle}{\langle \tilde{\rho}_{22}(p \rightarrow 0) \rangle}, \quad (10)$$

which expresses the asymmetry in probabilities of electronic escape through branches  $L$  (site 3) and  $M$  (site 2).

Generally the analytical results are cumbersome. Here we present only some special cases where it is possible to describe the main characteristics of the process. First, we assume the case where  $\varepsilon_2 = \varepsilon_3 = \varepsilon$ ,  $\Delta_2 = \Delta_3 = \mu_2 = 0$ ,  $\mu_3 = \mu$ . It means that we have only the energy level fluctuation on branch  $L$  at site 3. In this case parameter  $K$  has the form

$$K = \frac{J^4 + \Gamma(\Gamma^2 + \varepsilon^2) \left( \Gamma + \frac{\mu}{\hbar} \right) + J^2 \Gamma \left( 2\Gamma + \frac{\mu}{\hbar} \right)}{J^4 + 2J^2 \Gamma \left( \Gamma + \frac{\mu}{\hbar} \right) + \Gamma^2 \left( \Gamma^2 + \varepsilon^2 + 2\Gamma \frac{\mu}{\hbar} + \frac{\mu^2}{\hbar^2} \right)}. \quad (11)$$

We can see that as  $\Gamma \rightarrow \infty$   $K \approx 1$ . It means that when the electron escapes from the system very quickly the asymmetry of the electron distribution cannot be achieved. For very slow escape, when  $\Gamma \rightarrow 0$ , the system can achieve the steady state. The steady state is symmetric and so we have symmetric electron transfer with  $K \approx 1$ . Now we will analyze the case when all sites in the system have the same energy. If  $\varepsilon = 0$  we get

$$K = \frac{J^2 + \Gamma^2}{J^2 + \Gamma \left( \Gamma + \frac{\mu}{\hbar} \right)}. \quad (12)$$

For  $\Gamma \geq 0$  the parameter  $K$  has only the one extreme. The minimum is achieved when  $\Gamma = J$  and  $K$  is

$$K = \frac{2J}{2J + \frac{\mu}{\hbar}}. \quad (13)$$

If  $J \gg \mu/\hbar$  then  $K \approx 1$ . We get the symmetric electron transfer for any value of  $\Gamma$ . When  $J \ll \mu/\hbar$  we have  $K \approx 2J\hbar/\mu \ll 1$ . In this case we get the asymmetric electron transfer. The electron is transported mainly through branch  $M$  (site 2) where no fluctuation of the energy level exists.

In the second example we consider only the fluctuation of the hopping term between sites 1 and 3 on branch  $L$ . If  $\varepsilon_2 = \varepsilon_3 = \varepsilon$ ,  $\Delta_2 = \mu_2 = \mu_3 = 0$ ,  $\Delta_3 = \delta$  we get

$$K = \frac{A}{B}, \quad (14)$$

where

$$\begin{aligned} A &= 2J^6 \left( \Gamma + \frac{\delta}{\hbar} \right) + \Gamma \frac{\delta}{\hbar} \left( 2\Gamma + \frac{\delta}{\hbar} \right) \left( \Gamma^2 + 4\Gamma \frac{\delta}{\hbar} + \varepsilon^2 \right) \\ &\times \left[ \left( \Gamma + \frac{\delta}{\hbar} \right)^2 + \varepsilon^2 \right] \\ &+ J^4 \left( 4\Gamma^3 + 11\Gamma^2 \frac{\delta}{\hbar} + 17\Gamma \frac{\delta^2}{\hbar^2} + 4 \frac{\delta^3}{\hbar^3} + \varepsilon^2 \frac{\delta}{\hbar} \right) \\ &+ J^2 \Gamma \left( \Gamma + \frac{\delta}{\hbar} \right) \left( 2\Gamma^3 + 9\Gamma^2 \frac{\delta}{\hbar} + 24\Gamma \frac{\delta^2}{\hbar^2} + 8 \frac{\delta^3}{\hbar^3} \right) \\ &+ J^2 \varepsilon^2 \left( 2\Gamma^3 + 7\Gamma^2 \frac{\delta}{\hbar} + 9\Gamma \frac{\delta^2}{\hbar^2} + \frac{\delta^3}{\hbar^3} \right), \end{aligned}$$

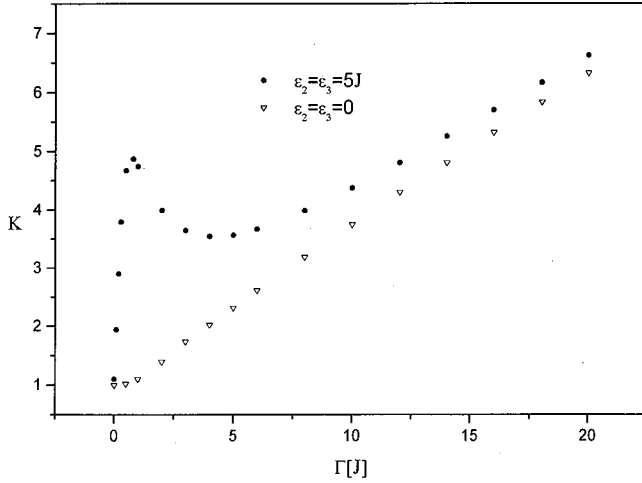


FIG. 3. The dependence of the ratio of electronic escape probabilities through the branch  $L$  and  $M$  ( $K$ ) on  $\Gamma$  with the parameters:  $J=1$ ,  $\mu_2/\hbar=0.005$ ,  $\mu_3/\hbar=0.005$ ,  $\Delta_2/\hbar=0.005$ ,  $\Delta_3/\hbar=0.3$ . Units are as described in the legend of Fig. 1.

$$B = J^2 \left( \Gamma + \frac{\delta}{\hbar} \right) \left[ J^2 + \Gamma \left( \Gamma + \frac{\delta}{\hbar} \right) \right] \left[ 2J^2 + \left( 2\Gamma + \frac{\delta}{\hbar} \right) \left( \Gamma + 4 \frac{\delta}{\hbar} \right) \right] + J^2 \varepsilon^2 \left[ J^2 \frac{\delta}{\hbar} + \left( \Gamma + \frac{\delta}{\hbar} \right)^2 \left( 2\Gamma + \frac{\delta}{\hbar} \right) \right].$$

In the case when  $\Gamma \rightarrow 0$   $K \cong 1$ . At this limit, as in the previous case, the system relaxes to the steady state while the electron is escaping from the system. When  $\Gamma \rightarrow \infty$  then  $K \rightarrow (\delta/\hbar J^2)\Gamma$ . This limit, in the case when  $\Delta_2 \neq 0$ , has the form  $K \sim \Delta_3/\Delta_2$ . With this limit the electron distribution in the system is developing from time zero highly asymmetrically. We get the asymmetric electron transfer through the system. The electron is transported mainly through the branch where the fluctuation of the hopping term is bigger. From Eqs. (11)–(14) it can be seen that  $K$  does not depend on the sign of the energy  $\varepsilon$ .

The dependence of  $K$  on  $\Gamma$  for some parameters which characterize our system is illustrated in Figs. 3–8. Figure 3 presents the influence of asymmetry in parameters  $\Delta_i$  on the electron transport. The electron is transferred mainly through the branch where  $\Delta_i$  is greater. The influence of asymmetry in parameters  $\mu_i$  on the ET is illustrated Fig. 4. If  $\varepsilon_i=0$  we get ET through the branch where  $\mu_i$  is smaller. When  $\varepsilon_2 = \varepsilon_3 \neq \varepsilon_1$  we can get ET through the branch with bigger  $\mu_i$ . The increase in the asymmetry of parameters  $\mu_i, \Delta_i$  increases the asymmetry in ET (Fig. 5). The same effect increases the energy difference between sites 2, 3, and 1 (Fig. 6).

The influence of energy difference between molecules on electron transfer asymmetry in the case of small fluctuations is presented in Fig. 7. The increase of the fluctuations causes the decrease of ET asymmetry in the case of asymmetric arrangement of energy levels (Figs. 7 and 8).

#### IV. DISCUSSION OF THE MODEL

From our analysis we can conclude that the fluctuation of the hopping term increases the electron transport in a particu-

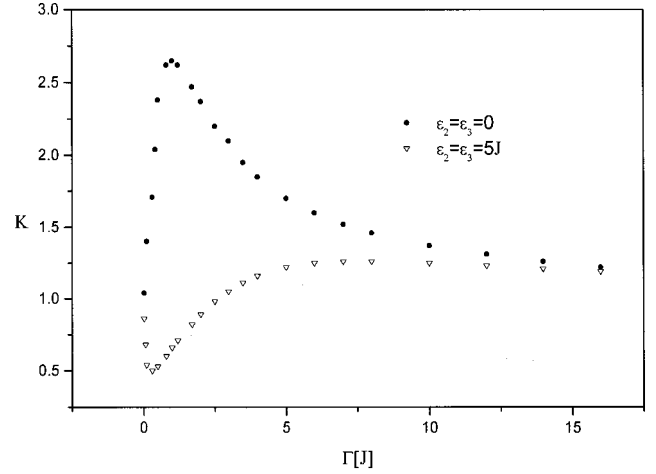


FIG. 4. The dependence of the ratio of electronic escape probabilities through the branch  $L$  and  $M$  ( $K$ ) on  $\Gamma$  with the parameters:  $J=1$ ,  $\mu_2/\hbar=5$ ,  $\mu_3/\hbar=0.5$ ,  $\Delta_2/\hbar=0.01$ ,  $\Delta_3/\hbar=0.01$ . Units are as described in the legend of Fig. 1.

lar direction. As a consequence is the fact that the branch with a larger  $\Delta_i$ , characterizing the size of fluctuation in interaction responsible for electron transfer in branch with  $i$ th molecule, has also a larger quantum yield  $\Phi_i$ .

The influence of the energy level fluctuation depends on the energy level differences between molecules. The quantum yield is smaller on the branch where the parameter  $\mu_i$ , characterizing the size of energy fluctuation at the  $i$ th molecule, is greater for the resonance case ( $\varepsilon_i=0$ ). In the non-resonant case, with a nonzero difference in the energy between sites 2, 3, and 1, the situation can be opposite. The quantum yield is higher in the branch with higher energy fluctuation and it is also dependent on the relations between  $\varepsilon_i$  and  $\mu_i$ .

The asymmetry is strongly dependent on the parameter  $\Gamma$ . When value of the parameter  $\Gamma$  is close to the  $J$  value then

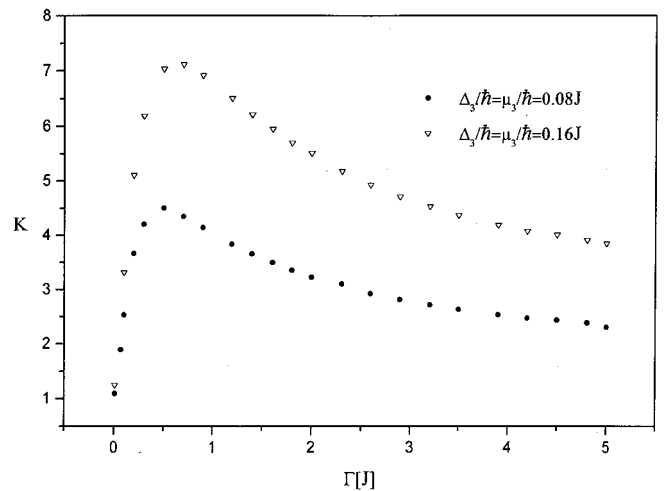


FIG. 5. The dependence of the ratio of electronic escape probabilities through the branch  $L$  and  $M$  ( $K$ ) on  $\Gamma$  with the parameters:  $J=1$ ,  $\varepsilon_2=10$ ,  $\varepsilon_3=10$ ,  $\mu_2/\hbar=0.01$ ,  $\Delta_2/\hbar=0.01$ . Units are as described in the legend of Fig. 1.

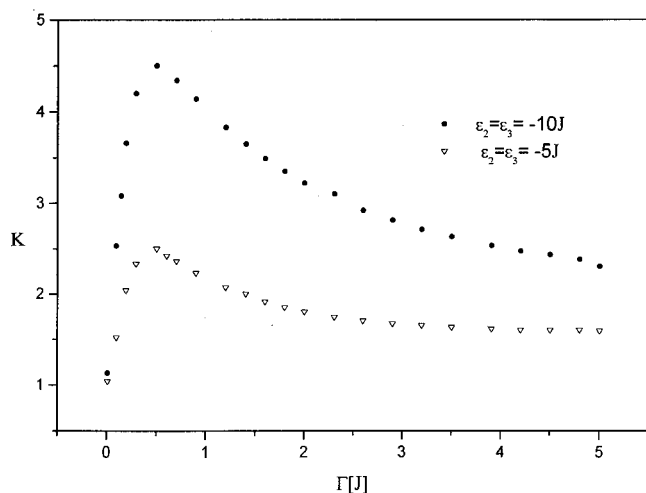


FIG. 6. The dependence of the ratio of electronic escape probabilities through the branch  $L$  and  $M$  ( $K$ ) on  $\Gamma$  with the parameters:  $J=1$ ,  $\mu_2/\hbar=0.01$ ,  $\mu_3/\hbar=0.08$ ,  $\Delta_2/\hbar=0.01$ ,  $\Delta_3/\hbar=0.08$ . Units are as described in the legend of Fig. 1.

the parameter  $K$ , describing the asymmetric quantum yield, has a local maximum.

For large  $\Gamma$  the parameter  $K$  achieves the value  $\Delta_3/\Delta_2$  which can be greater than its local maximum. By changing  $\Gamma$  we can choose the branch where the electron is transported with higher probability. Figure 4 illustrates the case with a small  $\Gamma$  when ET proceeds mainly through branch  $M$  and from some specific value of  $\Gamma$  the electron is transported with higher probability through branch  $L$ .

If we assume that the overall  $C_2$  symmetry is only approximate and there is a difference in energy levels between branch  $L$  and  $M$  we can get highly asymmetric ET. The interesting case is presented in Figs. 7 and 8 with the small fluctuation of parameters in the asymmetric arrangement of energy levels. The energy asymmetry of a few  $J$  (energy is measured in  $J$  units) can cause a strong asymmetry in ET

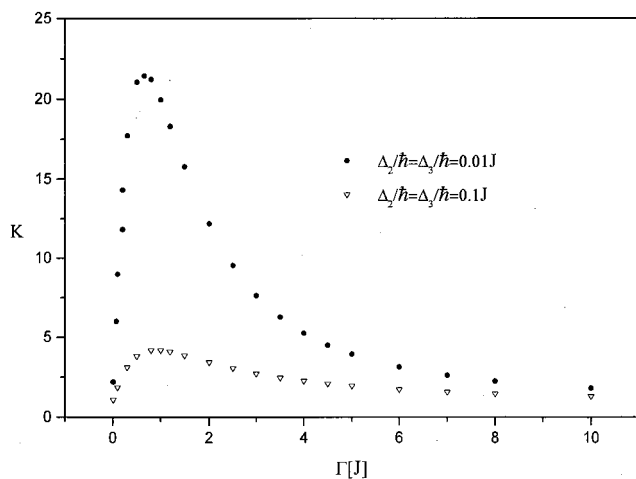


FIG. 7. The dependence of the ratio of electronic escape probabilities through the branch  $L$  and  $M$  ( $K$ ) on  $\Gamma$  for the parameters:  $J=1$ ,  $\varepsilon_2=10$ ,  $\varepsilon_3=0$ ,  $\mu_2/\hbar=\mu_3/\hbar=0.01$ . Units are as described in the legend of Fig. 1.

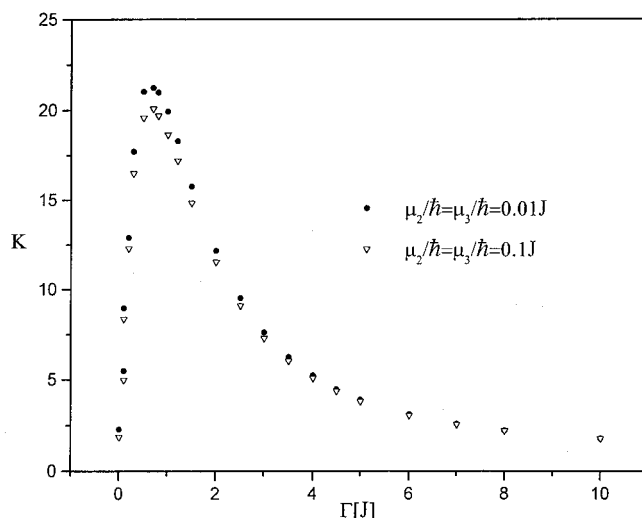


FIG. 8. The dependence of the ratio of electronic escape probabilities through the branch  $L$  and  $M$  ( $K$ ) on  $\Gamma$  with the parameters:  $J=1$ ,  $\varepsilon_2=10$ ,  $\varepsilon_3=0$ ,  $\Delta_2/\hbar=\Delta_3/\hbar=0.01$ . Units are as described in the legend of Fig. 1.

through the system for some parameter  $\Gamma$ . The fluctuation of the hopping term decreases strongly the asymmetry of ET through the system in the case when  $C_2$  symmetry is only approximate. The effect of the energy level fluctuation depends on the asymmetry arrangement of the energy level. Some value of the parameters which characterize the energy level fluctuation can increase the ET asymmetry, however, the larger value of the same parameters decreases the ET asymmetry.

Now we would like to apply our model to the primary charge transfer in the bacterial reaction center. Candidates for molecules 2 and 3 are the accessory BChl or some amino acid between  $P$  and BChl. Crystallography measurements indicate a higher mobility of the cofactors in the branch  $M$  [8]. If we want to elucidate the unidirectionality of the primary charge separation through the branch with lower mobility in the case of fully symmetric RC's we must consider the situation depicted in Fig. 4, the resonance case. The asymmetry is caused by the fluctuation of energy in the case of zero energy difference between sites 1, 2, and 3. In this case the electron is transported mainly through the branch with the smaller fluctuation of energy level. The fluctuation of hopping terms must be small. In this case we get the value for  $K\sim 2-3$ . Similar unidirectional asymmetry of electron transfer was measured in modified RC's [9].

To elucidate the higher asymmetry in an electron transfer in the case of exact  $C_2$  symmetry we must assume that there is the larger noise difference between branches  $L$  and  $M$ .

However, the overall  $C_2$  symmetry is only approximate in RC's. There are differences in the vicinity of prosthetic groups which can cause the differences in the energy level between molecules in branches  $L$  and  $M$ . In this case ET can be highly asymmetric (Figs. 7 and 8). Moreover, the position of atoms in the vicinity of the special pair  $P$  must also have a strong stability to get such high asymmetry. In some bacterial reaction centers the estimated value of the hopping

term was estimated to be  $J \sim 0.01$  eV (Ref. [12]) for primary charge transfer separation. The difference of a few hundredths of eV between energy levels can cause a high asymmetry in the quantum yield of electronic escape through the different branches. This energy difference can be caused by different environments of cofactors on branches  $L$  and  $M$ .

Using our model there are two ways to explain the unidirectionality of electron transfer in RC. The first one is a large difference of the noise on  $L$  and  $M$  side of RC's. The second one is a large difference in the energy levels of the accessory bacteriochlorophylls on the  $M$  and  $L$  branches of RC's.

## V. APPLICATION TO RC's

The analysis of amino acid mutations or cofactor modifications [9,30–37] that alter the highly asymmetric functionality of RC's can provide insight into the key factors impacting the directionality and the yield of electron transfer. In the literature are described cases in which ET to the  $L$  versus the  $M$  side in the RC was essentially modulated by changing several parameters. The drastically reduced quantum yield (QY) was observed in RC's where substantially different chromophores were in the binding pockets of the electron acceptors [35,36]. In a series of Rhodospirillum rubrum RC mutants [33] the  $G(M201)D/L(M212)H$  double mutant has 15% electron transfer to  $M$ -side bacteriochlorophyll, 70% of electron transfer to the  $L$ -side cofactors, and 15% was deactivated to the ground state. The changes in the ET directionality were explained by the raised free energy of  $P^+BChl_L^-$  in the interaction with Asp M201.

With a triple mutant  $S(L178)K/G(M201)D/L(M212)H$  62% of electron transfer was observed to the  $L$ -side BPh, 23% to the  $M$ -side BPh and 15% was returning to the ground state. In the case of triple mutants,  $S(L178)K/G(M201)D/L(M212)H$ , the  $S(L178)K$  mutation might lower a  $P^+BChl_M^-$  free energy and thus increases the yield of electron transfer to  $BPh_M$  in comparison to the  $G(M201)D/L(M212)H$  double mutant.

ET to the primary quinone in the normal  $\beta$ -type mutant was  $\sim 70\%$  and  $\sim 30\%$  was returning to the ground state [9,33]. The exact values depend on the specificity of mutation. The  $F(L121)D$  mutant exhibits beta type photochemistry [33]. It was proposed that  $P^+BChl_L^-$  lies at higher free energy in the  $F(L121)D$  mutant than in the wild-type (WT) RC.

The RC's of *Rb. sphaeroides* ( $M$ ) $H202L$  single mutant and ( $M$ ) $H202L/(L)L131H$  double mutant [34] contain a bacteriochlorophyll/bacteriochlorophyll heterodimer as a primary electron donor. These heterodimer mutants display a reduced yield of  $P^+Q_L^-$  formation for about 40% (single mutant) and 25% for the double mutants. This perturbation results from an upshift of the heterodimer free energy relative to homodimer primary donor of wild-type RC's. Electron transfer along the  $M$  side was observed in the  $H(M182)L$  mutant of *Rb. sphaeroides* [35]. In this mutant bacteriochlorophyll (referred to as  $\Phi_M$ ) is incorporated in place of  $BChl_M$ . One would expect that the  $P^+\Phi_M^-$  state would be considerably lower in energy than  $P^+BChl_M^-$ , thus enhancing the probability of  $M$ -side electron transfers.

The yield of the  $P^+\Phi_M^-$  state is apparently 30–40%.

The RC's of *Rhodospseudomonas viridis* mutant, where histidine was replaced by glutamate (denoted as  $L153HE$ ), the quantum yield of  $P^+Q_L^-$  formation is reduced to 75% [36]. In this mutant rise in the energy level of  $P^+BChl_L^-$  occurred because of the presence of glutamate. The exchange of histidine to leucine in RC's of *Rh. viridis* (the mutant denoted as  $L153HL$ ) causes the incorporation of a bacteriochlorophyll  $b$  instead of a bacteriochlorophyll  $a$  molecule (referred to as  $B_L$ ). As a consequence of the chromophore exchange the energy level of the electron transfer state  $P^+B_L^-$  is lowered in comparison to  $P^+BChl_L^-$  (WT). Consequently the quantum yield of  $P^+B_L^-$  is reduced to 50% in this mutant [36].

The presented experimental data show that the free energy of the intermediates  $P^+BChl_L^-$  and  $P^+BChl_M^-$  does have a major importance. If the free energy of  $P^+BChl_L^-$  is raised relative to that of the wild-type RC (e.g., by the introduction of a negative charge like in the mutant  $L153HE$ ) the quantum efficiency is considerably lowered.

The implementation of the theory requires information regarding the energetic parameters such as the energy gap of the equilibrium nuclear configuration between  $P^*$  and  $P^+BChl_{L(M)}^-$ . The energy level of  $P^+BChl_L^-$  in RC's of *Rb. Sphaeroides* is about  $450\text{ cm}^{-1}$  below the  $P^*$  state [37]. Another calculation shows that this energy level is about  $250\text{ cm}^{-1}$  above the special pair [38]. Theoretical calculation using the *Rh. viridis* RC crystal structure suggested that the  $P^+BChl_M^-$  state is  $2000\text{ cm}^{-1}$  higher than  $P^*$  [39].

The other parameters included in our model are imaginary part of energy levels  $\Gamma_1, \Gamma_2, \Gamma_3$ . The value of  $\Gamma_1$  is calculated from the internal conversion rate of  $P^*$ . This rate was estimated to be between  $(90\text{ ps})^{-1}$  and  $(350\text{ ps})^{-1}$  from the measurements on WT RC's [34]. For our theoretical simulations the internal conversion rate of  $(130\text{ ps})^{-1}$  was selected. Then the parameter  $\Gamma_1$ , characterizing the decay of the system to the ground state, is obtained from expression  $2\Gamma_1/\hbar \approx (130\text{ ps})^{-1}$ . The values of parameters  $\Gamma_2, \Gamma_3$  can be calculated in a similar way from the decay time of  $P^+BChl_L^-$ . The decay time of  $P^+BChl_L^-$  in *Rhodospseudomonas viridis* is  $0.65\text{ ps}$  (Ref. [37]) and the transfer integral  $J$  is estimated to be about  $20\text{ cm}^{-1}$  [40–42].

To characterize the wild-type RC in our model the following parameters were chosen: the energy levels  $\varepsilon_2 = 2000\text{ cm}^{-1}$ ,  $\varepsilon_3 = 400\text{ cm}^{-1}$ , hopping term  $J = 20\text{ cm}^{-1}$ , imaginary part of energy levels  $\Gamma_2 = \Gamma_3 = \Gamma = 4\text{ cm}^{-1}$  [ $2\Gamma/\hbar \approx (0.65\text{ ps})^{-1}$ ]. Similarly to the work of Ref. [40] it was assumed that  $\Gamma_1$  is smaller by about two orders of magnitude than the  $\Gamma_2$  and  $\Gamma_3$ . This assumption has the experimental support [34,37]. The parameters characterizing the noise and the decay of the system to the ground state were:  $\mu_2/\hbar = \mu_3/\hbar = 200\text{ cm}^{-1}$ ,  $\Delta_2/\hbar = \Delta_3/\hbar = 0$ , and  $\Gamma_1 = 2 \cdot 10^{-2}\text{ cm}^{-1}$  for WT RC's. It has to be noticed that QY in our model does not depend on the sign of the energy levels  $\varepsilon_2, \varepsilon_3$  and we also assume that the hopping terms do not fluctuate.

Using the above parameters the following quantum yields were obtained for wild-type RC's:  $\Phi_1 = 0.05$ ,  $\Phi_2 = 0.05$ ,

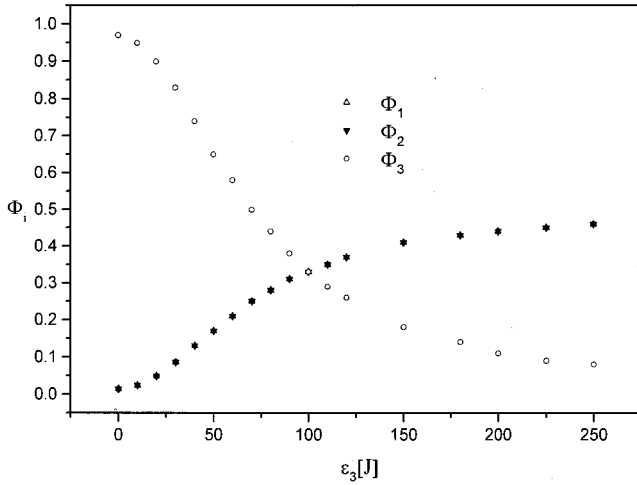


FIG. 9. The dependence of charge separation quantum yields  $\Phi_i$  ( $i=1,2,3$ ) on  $\varepsilon_3$  energy. Parameters used for simulation:  $J=1$ ,  $\varepsilon_2=100$ ,  $\mu_2/\hbar=\mu_3/\hbar=10$ ,  $\Delta_2/\hbar=\Delta_3/\hbar=0$ ,  $\Gamma_2=\Gamma_3=0.2$ , and  $\Gamma_1=0.001$ . Units are as described in the legend of Fig. 1.

$\Phi_3=0.9$ . If we assume the asymmetry in the noise characterizing parameter and the value of parameter  $\Gamma_1$  is taken to be equivalent to the internal conversion rate  $(130 \text{ ps})^{-1}$  then with  $\mu_2/\hbar=0$ ,  $\mu_3/\hbar=200 \text{ cm}^{-1}$  the quantum yields are:  $\Phi_1=0.05$ ,  $\Phi_2=0.001$ ,  $\Phi_3=0.949$ . Even if the  $\Gamma_1$  value in calculation is greater than average we will get a relatively high quantum yield to ground state.

Based on our model Figs. 9 and 10 present the dependence of the quantum yields on the energy gaps between  $P^*$  and  $P^+BChl_{L(M)}^-$ . These figures describe the mutated RC's, where the mutation changed the relative free energies of the participating states.

When the energy of  $\varepsilon_3$  is increased, as in the  $G(M201)D/L(M212)H$  double mutant comparing to WT RC's, we have QY:  $\Phi_1=0.14$ ,  $\Phi_2=0.14$ ,  $\Phi_3=0.72$  with the parameters:  $\varepsilon_2=2000 \text{ cm}^{-1}$ ,  $\varepsilon_3=800 \text{ cm}^{-1}$ ,  $J=20 \text{ cm}^{-1}$ ,

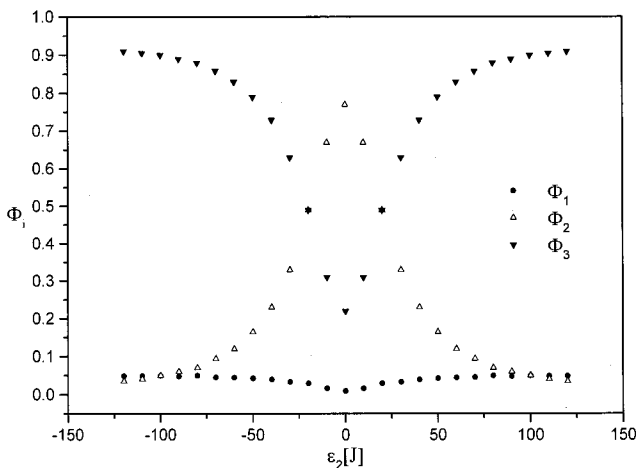


FIG. 10. The dependence of charge separation quantum yields  $\Phi_i$  ( $i=1,2,3$ ) on  $\varepsilon_2$  energy. Parameters used for simulation:  $J=1$ ,  $\varepsilon_3=20$ ,  $\mu_2/\hbar=\mu_3/\hbar=10$ ,  $\Delta_2/\hbar=\Delta_3/\hbar=0$ ,  $\Gamma_2=\Gamma_3=0.2$ , and  $\Gamma_1=0.001$ . Units are as described in the legend of Fig. 1.

$\Gamma_2=4 \text{ cm}^{-1}$ ,  $\Gamma_3=0.8 \text{ cm}^{-1}$ ,  $\mu_2/\hbar=\mu_3/\hbar=200 \text{ cm}^{-1}$ ,  $\Delta_2/\hbar=\Delta_3/\hbar=0$ , and  $\Gamma_1=2.10^{-2} \text{ cm}^{-1}$ . The smaller value of parameter  $\Gamma_3$  in comparison to WT is justified by the experimental data [9,33].

When the energy of  $\varepsilon_2$  is decreased, as in  $S(L178)K/G(M201)D/L(M212)H$  triple mutant in comparison with the double mutant we have QY:  $\Phi_1=0.13$ ,  $\Phi_2=0.20$ ,  $\Phi_3=0.67$  using the parameters:  $\varepsilon_2=1600 \text{ cm}^{-1}$ ,  $\varepsilon_3=800 \text{ cm}^{-1}$ ,  $J=20 \text{ cm}^{-1}$ ,  $\Gamma_2=4 \text{ cm}^{-1}$ ,  $\Gamma_3=0.8 \text{ cm}^{-1}$ ,  $\mu_2/\hbar=\mu_3/\hbar=200 \text{ cm}^{-1}$ ,  $\Delta_2/\hbar=\Delta_3/\hbar=0$ , and  $\Gamma_1=2.10^{-2} \text{ cm}^{-1}$ .

When the energy  $\varepsilon_2$  is considerably decreased in comparison to WT as in the  $H(M182)L$  mutant of Rb sphaeroides where bacteriopheophytin is incorporated in place of  $BChl_M$  we get the following QY:  $\Phi_1=0.04$ ,  $\Phi_2=0.33$ ,  $\Phi_3=0.63$  by using the parameters:  $\varepsilon_2=-600 \text{ cm}^{-1}$ ,  $\varepsilon_3=400 \text{ cm}^{-1}$ ,  $J=20 \text{ cm}^{-1}$ ,  $\Gamma_2=4 \text{ cm}^{-1}$ ,  $\Gamma_3=4 \text{ cm}^{-1}$ ,  $\mu_2/\hbar=\mu_3/\hbar=200 \text{ cm}^{-1}$ ,  $\Delta_2/\hbar=\Delta_3/\hbar=0$ , and  $\Gamma_1=2.10^{-2} \text{ cm}^{-1}$ .

When the energy  $\varepsilon_3$  is sufficiently decreased in comparison to WT as in the  $L153HL$  mutant of Rh viridis where bacteriopheophytin is incorporated in place of  $BChl_L$  we have the following QY:  $\Phi_1=0.12$ ,  $\Phi_2=0.44$ ,  $\Phi_3=0.44$  with the parameters:  $\varepsilon_2=2000 \text{ cm}^{-1}$ ,  $\varepsilon_3=-2000 \text{ cm}^{-1}$ ,  $J=20 \text{ cm}^{-1}$ ,  $\Gamma_2=4 \text{ cm}^{-1}$ ,  $\Gamma_3=4 \text{ cm}^{-1}$ ,  $\mu_2/\hbar=\mu_3/\hbar=200 \text{ cm}^{-1}$ ,  $\Delta_2/\hbar=\Delta_3/\hbar=0$ , and  $\Gamma_1=6.10^{-3} \text{ cm}^{-1}$ . The parameter  $\Gamma_1$  in comparison with RC's of other bacteria was lowered. Our value of  $\Gamma_1$  correspond to value of  $(390 \text{ ps})^{-1}$  for the  $P^*$  internal conversion rate which is relatively small. The higher value of this parameter causes the strong decay to the ground state. It means that the difference between  $\varepsilon_1$  and  $\varepsilon_2$ ,  $\varepsilon_3$  ought to be smaller.

The normal  $\beta$ -type mutant was not analyzed because of the strong possibility that electron is also delocalized on the  $BChl(\beta)$  which is incorporated in the place of  $BPh_L$ . This possibility is not incorporated in our model. And in the case of the heterodimer mutant it is not obvious how the electron levels might be shifted and without this information it is difficult to make the simulations.

## VI. CONCLUSION

The present study addresses the important problem of the highly asymmetric ET in the photosynthetic reaction centers. Using the stochastic model it was possible to elucidate the unidirectionality of electron transfer. In the model the electron is delocalized to the three molecules ( $P$ ,  $BChl_L$ , and  $BChl_M$ ) with the electron density dependent on the parameters characterizing the system. The electron density in this system can be strongly asymmetric and the energy levels of the  $BChl_L$  and  $BChl_M$  molecules have been shown to influence profoundly the asymmetry.

We have shown that in mutations of RC's where the difference between energy levels  $\varepsilon_2$  and  $\varepsilon_1$  are increased in comparison with wild type, the unidirectionality of electron transfer is also increased. The same effect is observed for the decrease of the energy level difference between  $\varepsilon_3$  and  $\varepsilon_1$ .

The results demonstrate that an individual amino acid

residue can, through its influence on the free energy of the charge-separated states, effectively dictate the balance between the ET to the  $L$ - and  $M$ -side chromophores of the RC's.

In the present work the temperature dependence of ET was not analyzed. Nevertheless, we would like to say few words about the temperature effect. A noise which influences the asymmetric ET in the present analysis is dependent on the temperature. It would be interesting to know whether the unidirectionality of the primary charge separation process in RC's is temperature dependent. The primary processes in photosynthetic reaction centers have the anomalous temperature dependence. This dependence can be explained by the inclusion of the relative motion of exchanging groups into the electron-transport theory [43]. The main effect will be the temperature dependence of  $J$  [43,44]. Because the parameter  $\Gamma$  can also be dependent on the temperature there is a possibility to change the asymmetry of ET in RC's with a temperature.

However, the primary electron transfer reactions in RC's have the slight temperature dependence. The charge separation time constant decreases only two to three times on cooling from 300 to 10 K [8]. If consequently the parameter  $\Gamma$  is changed two times in the vicinity of maximum asymmetry ( $\Gamma \sim J$ ) there is no sufficient change in asymmetry of ET. As a result we have a small temperature dependence of asymmetry in electron transfer in the RC's. Also in the case of small fluctuations the asymmetry of ET through the system is temperature independent. When  $\Gamma \ll \varepsilon_L$  and  $\varepsilon_M$  then the several times increase or decrease of parameter  $\Gamma$  does not affect strongly the asymmetry of ET and its temperature dependence.

It was shown that the different hopping terms (electron-transfer integrals) in the branches can result in the asymmetry of charge separation across the  $L$  and  $M$  branches of the RC [45,46]. However, the present work demonstrates that for

the asymmetric ET it is not sufficient to consider only an asymmetry in electron-transfer integrals. For example, in the case of small  $\Gamma$ , the system approaches to the quasisteady state, where asymmetry is determined by equilibrium electron density distribution and does not depend on electron-transfer integral.

For example there is a mutant of RC's where hopping integrals are not changed significantly and yet the unidirectionality is suppressed considerably [33]. It is in contradiction to the work [47] where the unidirectionality was explained only on the basis of the asymmetry of transfer integrals in the  $L$  and  $M$  regions. It was suggested also that the dimer of RC's plays the decisive role for the vectorial charge separation [48]. However, this explanation is in a contrast to the experimental data. The profound changes in the unidirectionality of ET were observed for some mutants of RC's without the changes in the aggregation state [9,33,36].

The present study demonstrates that the energy levels of the accessory bacteriochlorophyll play the critical role in the unidirectionality of the primary electron transfer. Despite the crucial role of the accessory bacteriochlorophylls for the asymmetric ET the overall reaction required certain relation among the parameters describing the whole system. The most important conclusion from the present study is that to achieve the high asymmetry of ET it is not sufficient to describe the isolated ET between primary donor and accessory bacteriochlorophylls. To achieve the asymmetric ET it is also necessary to take into account the effect of the next ET step. It means that reaction centers are the complex system where a one step in ET is coupled to the next step to get the maximal efficiency in its functionality.

#### ACKNOWLEDGMENTS

We thank Dr. M. Fabian and Dr. V. Lisy for useful comments. This work has been supported by the Slovak Scientific Grant Agency, Grant No. 7043.

- 
- [1] J. Deisenhofer, O. Epp, K. Miki, R. Huber, and H. Michel, *J. Mol. Biol.* **180**, 385 (1984).
  - [2] H. Michel, O. Epp, and J. Deisenhofer, *EMBO J.* **5**, 2445 (1986).
  - [3] L. N. M. Duysens, *Biochim. Biophys. Acta* **19**, 188 (1956).
  - [4] H. Michel, K. A. Weyer, H. Gruenberg, and F. Lottspeich, *EMBO J.* **4**, 1667 (1985).
  - [5] K. A. Weyer, F. Lottspeich, H. Gruenberg, F. S. Lang, D. Oesterhelt, and H. Michel, *EMBO J.* **6**, 2197 (1987).
  - [6] J. Deisenhofer and H. Michel, *EMBO J.* **8**, 2149 (1989).
  - [7] J. L. Martin, J. Breton, A. J. Hoff, A. Migus, and A. Antonetti, *Physica A* **83**, 957 (1986).
  - [8] A. J. Hoff and J. Deisenhofer, *Phys. Rep.* **287**, 1 (1997).
  - [9] B. A. Heller, D. Holten, and C. Kirmaier, *Science* **269**, 940 (1995).
  - [10] C. Kirmaier and D. Holten, *Proc. Natl. Acad. Sci. U.S.A.* **87**, 3552 (1990).
  - [11] E. Takahashi and C. A. Wraight, *Biochemistry* **31**, 855 (1992).
  - [12] V. A. Shuvalov and L. N. M. Duysens, *Proc. Natl. Acad. Sci. U.S.A.* **83**, 1690 (1986).
  - [13] J. N. Gehlen, M. Marchi, and D. Chandler, *Science* **263**, 499 (1994).
  - [14] H. Haken and P. Reineker, *Z. Phys.* **249**, 253 (1972).
  - [15] P. Reineker, B. Kaiser, and A. M. Jayannavar, *Phys. Rev. A* **39**, 1469 (1989).
  - [16] A. Blumen and R. Silbey, *J. Chem. Phys.* **69**, 3589 (1978).
  - [17] V. Čápek and V. Szös, *Phys. Status Solidi B* **131**, 667 (1985).
  - [18] D. W. Brown, K. Lindenberg, and B. J. West, *J. Chem. Phys.* **83**, 4136 (1985).
  - [19] M. Pudlak, *Chem. Phys. Lett.* **235**, 126 (1995).
  - [20] M. Pudlak, *Chem. Phys. Lett.* **221**, 86 (1994).
  - [21] M. Pudlak, *Czech. J. Phys.* **48**, 293 (1998).
  - [22] V. Čápek and V. Szöcs, *Phys. Status Solidi B* **125**, K137 (1984).
  - [23] P. Chvosta and I. Barvik, *Z. Phys. B: Condens. Matter* **85**, 227 (1991).
  - [24] V. M. Kenkre and P. Reineker, *Exciton Dynamics in Molecular Crystals and Aggregates*, Springer Tracts in Modern Physics Vol. 94 (Springer, Berlin, 1982).

- [25] A. A. Ovchinnikov, S. F. Timashev, and A. A. Bely, *Kinetics of Diffusion Controlled Chemical Processes* (Nova Science, Commack, NY, 1989).
- [26] V. I. Klyatskin, *Statisticeskoe Opisanie Dinamiceskich Sistem s Fluktuirujuscimi Parametrami* (Nauka, Moskva, 1975).
- [27] P. Hänggi, *Z. Phys. B* **31**, 407 (1978).
- [28] M. Pudlak, *J. Chem. Phys.* **108**, 5621 (1998).
- [29] J. Jortner, S. A. Rice, and R. M. Hochstrasser, *Radiationless Transitions in Photochemistry*, *Advances in Photochemistry* Vol. 7 (Wiley, New York, 1969), p. 149.
- [30] S. Lin, J. E. Eastman, A. K. W. Taguchi, and N. W. Woodbury, *Biochemistry* **35**, 3187 (1996).
- [31] A. K. W. Taguchi, J. E. Eastman, D. M. Gallo, E. Sheagley, W. Xiao, and N. W. Woodbury, *Biochemistry* **35**, 3175 (1996).
- [32] M. E. Van Brederode, M. R. Jones, F. Van Mourik, I. H. M. Van Stokkum, and R. Van Grondelle, *Biochemistry* **36**, 6855 (1997).
- [33] Ch. Kirmaier, D. Weems, and D. Holten, *Biochemistry* **38**, 11 516 (1999).
- [34] L. L. Laporte, V. Palaniappan, D. G. Davis, Ch. Kirmaier, C. C. Schenck, D. Holten, and D. F. Bocian, *J. Phys. Chem.* **100**, 17 696 (1996).
- [35] E. Katilius, T. Turanchik, S. Lin, A. K. W. Taguchi, and N. W. Woodbury, *J. Phys. Chem. B* **103**, 7386 (1999).
- [36] T. Artl, B. Dohse, S. Schmidt, J. Wachtveitl, E. Laussermair, W. Zinth, and D. Oesterhelt, *Biochemistry* **35**, 9235 (1996).
- [37] T. Artl, M. Bibikova, H. Penzkofer, D. Oesterhelt, and W. Zinth, *J. Phys. Chem.* **100**, 12 060 (1996).
- [38] M. R. A. Blomberg, P. E. M. Siegbahn, and G. T. Babcock, *J. Am. Chem. Soc.* **120**, 8812 (1998).
- [39] W. W. Parson, Z. T. Chu, and A. Warshel, *Biochim. Biophys. Acta* **1017**, 251 (1990).
- [40] S. Tanaka and R. A. Marcus, *J. Phys. Chem. B* **101**, 5031 (1997).
- [41] E. Sim and N. Makri, *J. Phys. Chem. B* **101**, 5446 (1997).
- [42] R. A. Marcus, *Chem. Phys. Lett.* **133**, 471 (1987).
- [43] M. Pudlak and K. V. Shaitan, *J. Biol. Phys.* **19**, 39 (1993).
- [44] I. A. Goyuchuk, E. G. Petrov, and V. May, *J. Chem. Phys.* **103**, 4937 (1995).
- [45] M. Plato, K. Möbius, M. E. Michel-Beyerle, M. Bixon, and J. Jortner, *J. Am. Chem. Soc.* **110**, 7279 (1988).
- [46] M. Bixon, J. Jortner, and M. E. Michel-Beyerle, *Biochim. Biophys. Acta* **1056**, 301 (1991).
- [47] J. Hasegawa and H. Nakatsuji, *J. Phys. Chem. B* **102**, 10 420 (1998).
- [48] P. O. J. Scherer, C. Scharnagl, and S. F. Fischer, *Chem. Phys.* **197**, 333 (1995).